Available online at www.sciencedirect.com
ScienceDirect
Thin Solid Films 515 (2007) 3840–3843
www.elsevier.com/locate/tsf

Transparent conducting yttrium-doped ZnO thin films deposited by sol–gel method

Qingjiang Yu, Haibin Yang *, Wuyou Fu, Lianxia Chang, Jing Xu, Cuiling Yu, Ronghui Wei, Kai Du, Hongyang Zhu, Minghui Li, Guangtian Zou

National Laboratory of Superhard Materials, Jilin University, Changchun, 130012, PR China

Received 28 March 2006; received in revised form 20 September 2006; accepted 13 October 2006
Available online 27 November 2006

Abstract

Transparent and conductive high preferential *c*-axis oriented ZnO thin films doped with yttrium have been prepared by sol–gel method using zinc acetate and yttrium chloride as cations source, 2-methoxyethanol as solvent and monoethanolamine (MEA) as sol stabilizer. Film deposition was performed by dip-coating technique at a withdrawal rate of 6.0 cm/min on silica glass substrates. The effect of dopant (Y) concentration, heating treatment and annealing in a reducing atmosphere on the structure, morphology, electrical and optical properties of ZnO thin films were investigated. When compared with the resistivity values of films without the annealing treatment, the values of films annealed in the reducing atmosphere were decreased by about three orders of magnitude. The lowest resistivity value was 6.75×10^{-3} Ω cm, which was obtained in the 0.5 at.% yttrium-doped ZnO thin film annealed in nitrogen with 5% hydrogen at 500 °C. The average optical transmittance values of the annealed films were more than 80% in the visible range. The energy band gap calculated from the transmittance spectra is about 3.30–3.37 eV.

Keywords: Zinc oxide; Thin film; Sol–gel method

1. Introduction

ZnO thin films have been extensively studied due to their potential applications in electronic and optoelectronic devices. ZnO thin films with preferential orientation along the *c*-axis have been demonstrated to operate as surface acoustic wave devices because of their large piezoelectric constant [1]. Transparent ZnO thin films can be doped with Al, Ga, In, etc. to tune their electrical conductivities for various electrical and optical applications including transparent conducting oxide electrodes for displays [2] and photovoltaic devices [3]. In addition, owing to their better stability in hydrogen plasma than that of indium tin oxide, ZnO thin films can be used in the fabrication of hydrogenated amorphous silicon solar cells [4].

ZnO thin films have been prepared by a variety of thin film deposition techniques, such as magnetron sputtering [5,6], pulsed laser deposition [7], chemical vapor deposition [8,9], reactive electron beam evaporation [10], spray pyrolysis [11,12] and sol–gel process [13–17], etc. Among them, the sol–gel technique is becoming more popular due to its simplicity, safety and low cost. Moreover, in the technique, incorporation of dopants is easy and large area substrates can be coated readily.

Highly transparent and conductive ZnO thin films have been prepared by doping with a group III impurity, such as Al, Ga or In, using sol–gel process [14–16]. Especially, a number of works have been carried out on aluminum-doped ZnO thin films by sol–gel method. Ohyama et al. [14] in their excellent work reported the preparation of aluminum-doped ZnO thin films with highly preferential crystal orientation by the sol–gel dip-coating method. They systematically investigated the effects of aluminum doping concentration and preparation conditions on the electrical resistivity of the gel-derived films. They reported the lowest resistivity of 6.5×10^{-3} Ω cm for the 0.5 at.% aluminum-doped films. However, highly transparent and conductive yttrium-doped ZnO thin films deposited by the sol–gel dip-coating method have not been reported before. In this work, the effect of dopant concentration, heating treatment

* Corresponding author. Tel.: +86 431 5168763; fax: +86 431 5168816.
E-mail address: yanghb@jlu.edu.cn (H. Yang).

0040-6090/$ - see front matter © 2006 Elsevier B.V. All rights reserved.
doi:10.1016/j.tsf.2006.10.077

and annealing in a reducing atmosphere on the structure, morphology, electrical and optical properties of ZnO thin films deposited on silica glass substrates by sol–gel method are investigated.

2. Experimental details

ZnO thin films were deposited on silica glass substrates by sol–gel method. Zinc acetate dihydrate ($Zn(CH_3COO)_2{\cdot}2H_2O$), 2-methoxyethanol and MEA were used as a starting material, solvent and sol stabilizer, respectively. The dopant source of yttrium was yttrium chloride (YCl_3). Zinc acetate dihydrate and yttrium chloride were first dissolved in a mixture of 2-methoxyethanol and MEA solution at room temperature. The molar ratio of MEA to zinc acetate ($Zn(CH_3COO)_2$) was maintained at 1.0 and the concentration of zinc acetate was 0.5 M. The resultant solution was stirred at 60 °C for 2 h to yield a clear and homogeneous solution, which served as the precursor solution after cooling to room temperature.

The dip-coating process was achieved when cleaned glass substrates were gradually immersed into the solution, remaining inside about 30 s and then withdrew at a rate of 6.0 cm/min at room temperature. After being deposited by dip coating, the films were dried at 300 °C for 10 min to evaporate the solvent and remove organic residuals. The procedures from coating to drying were repeated ten times until the thickness of the sintered films was approximately 300 nm. The films were then inserted into a furnace and fired in air at 300–550 °C for 2 h (the first post-heat treatment), followed by annealing in nitrogen with 5% hydrogen at 500 °C for 1 h (the second post-heat treatment).

The crystalline phase and crystallite orientation were determined by a Rigaku-2400 X-ray diffractometer (XRD) with CuKα radiation. The surface and cross-section of the films were observed with a field-emission scanning electron microscope (FE-SEM) (JEOL JSM-6700F). The electrical resistance was measured by a four-point probe method. Optical transmittance measurements were carried out using a UV-3150 double-beam spectrophotometer.

3. Results and discussion

3.1. Structural analysis

Fig. 1 shows XRD patterns of the 0.5 at.% yttrium-doped ZnO thin films heated at different temperature. It is found that the annealing temperature plays an important role in determining the crystal structure of ZnO thin films. The films (a–d) deposited at the first post-heat treatment temperature showed preferred ZnO (0 0 2) orientation, while the intensities of (0 0 2) peaks increased with an increase in the annealing temperature. This means that, the higher the annealing temperature, the higher the crystal quality. According to Ohyama et al. [17], the addition of MEA is effective in the formation of sol–gel ZnO films with a high degree of orientation along the (0 0 2) plane, while the effect of other stabilizers such as diethanolamine is to reduce the (0 0 2) preferential growth. These results are in accordance with the reports by other authors [16–19].

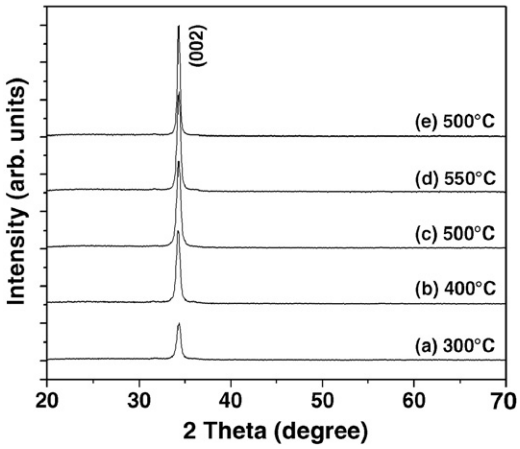

Fig. 1. XRD patterns of the 0.5 at.% yttrium-doped ZnO thin films dried at 300 °C and then heated at various temperatures ((a–d): the first post-heat treatment temperature and (e): the second post-heat treatment temperature with the first post-heat treatment at 550 °C).

Then the film which had the highest (0 0 2) peak intensity was heated in nitrogen with 5% hydrogen at 500 °C for 1 h (the second post-heat treatment). Compared with the (0 0 2) peak intensity of film (d) without the second post-heat treatment, that of film (e) with the second post-heat treatment was increased.

3.2. Morphological characteristics

Fig. 2 shows FE-SEM images of the surface and cross-section of the 0.5 at.% yttrium-doped ZnO thin films annealed at various temperatures (the first post-heat treatment temperatures (a–d) and the second post-heat treatment temperatures (e and f) with the first post-heat treatment at 550 °C). In the cases of films (a–d) with the first post-heat treatment, a granular and porous structure could be seen for all temperatures. As grains grew and agglomerated with an increase in the growth temperature, the nanoparticles gradually coalesced and formed the interparticle necks. The increased interparticle contacts are a prerequisite for obtaining good electrical conductivity in the final thin film [20]. Compared with film (d) without the second post-heat treatment, film (e) with the second post-heat treatment became larger and denser. Columnar ZnO crystals, which grew together between layers and layers and formed a seriate whole, and the films thickness of about 300 nm were observed in the cross-section image of the film (f).

3.3. Electrical properties

Fig. 3 shows electrical resistivity variations of the yttrium-doped ZnO thin films as a function of yttrium doping concentration. Without regard to the second post-heat treatment, the lowest electrical resistivity value of yttrium-doped films was obtained at 0.5 at.%. Non-stoichiometric ZnO thin film is known to be an n-type semiconductor with carriers (electrons) which are thermally excited from donor levels formed by interstitial zinc atoms or oxygen vacancies. The electrical resistivity of yttrium-doped ZnO thin films is lower than that of

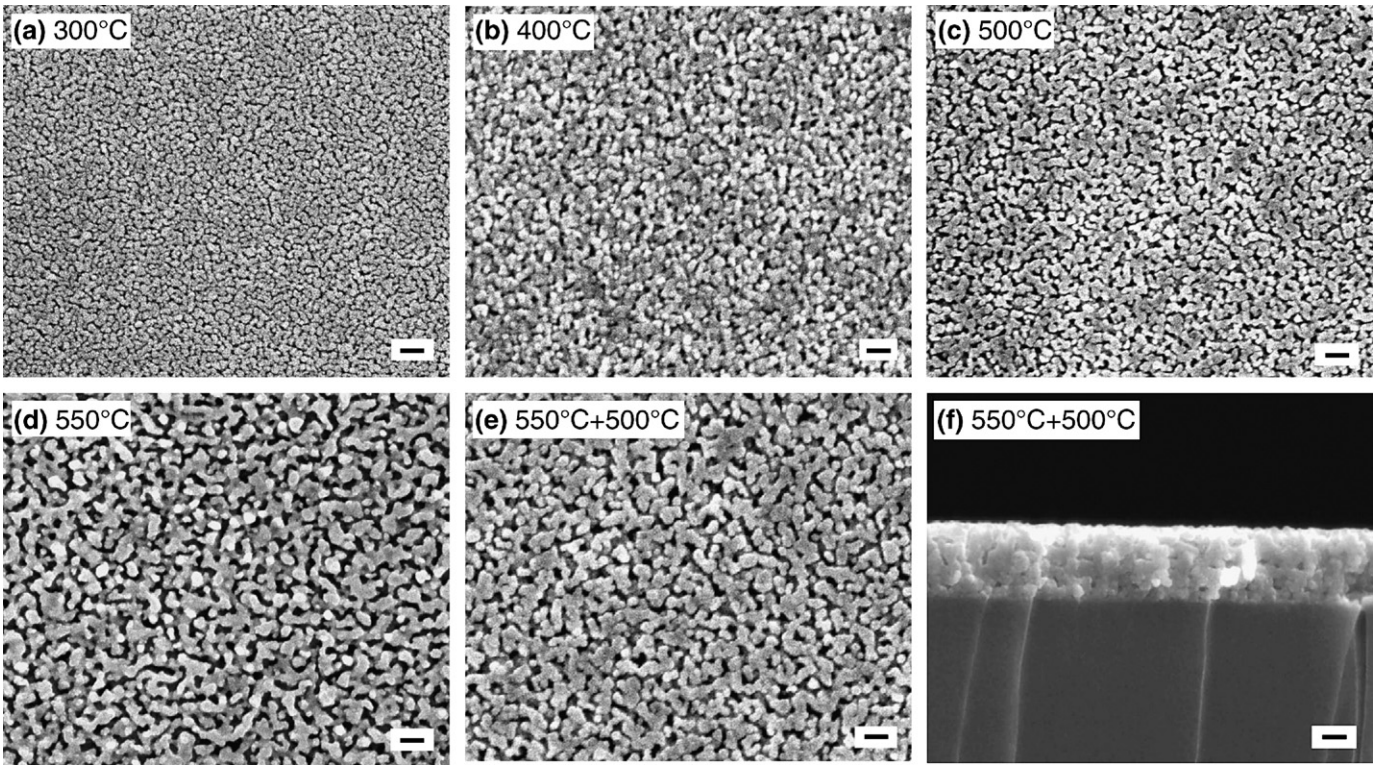

Fig. 2. FE-SEM images of the surface and cross-section of the 0.5 at.% yttrium-doped ZnO films dried at 300 °C and then heated at various temperatures ((a–d): the first post-heat treatment temperature and (e and f): the second post-heat treatment temperature with the first post-heat treatment at 550 °C). All scale bars are 100 nm.

undoped ZnO thin films due to the contribution of extra free carriers of Y^{3+} ions substituting Zn^{2+} ions. However, the electrical resistivity of doped films increased with increasing doping concentration, which may be due to a decrease in mobility of carriers caused by segregation of dopants at the grain boundary [18].

The lowest electrical resistivity value of films with the first post-heat treatment at 550 °C was approximately a few Ω cm, but when the second post-heat treatment was carried out in nitrogen with 5% hydrogen at 500 °C, it dropped by about three orders of magnitude and reached 6.75×10^{-3} Ω cm. Since the electrical conductivity of ZnO is directly related to the number of electrons, electrons formed by the ionization of the interstitial zinc atoms and the oxygen vacancies affect the electrical conductivity of ZnO crystals. The decrease in resistivity of films with the second post-heat treatment was affected by both the abovementioned cases but may be predominated by oxygen vacancies. This is because the oxygen vacancies formed by oxygen annihilation from the ZnO crystals via the annealing process in a reducing atmosphere [21]. In addition, when the second post-heat treatment is performed in a reducing atmosphere, the carrier's concentration may increase by desorption

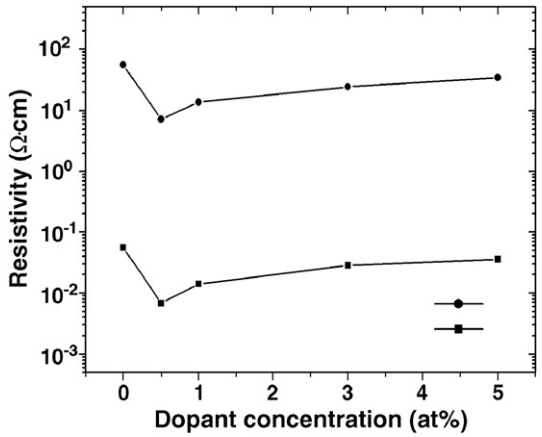

Fig. 3. Electrical resistivity of the yttrium-doped ZnO thin films as a function of yttrium doping concentration, the first post-heat treatment at 550 °C (●), the second post-heat treatment with the first post-heat treatment at 550 °C (■).

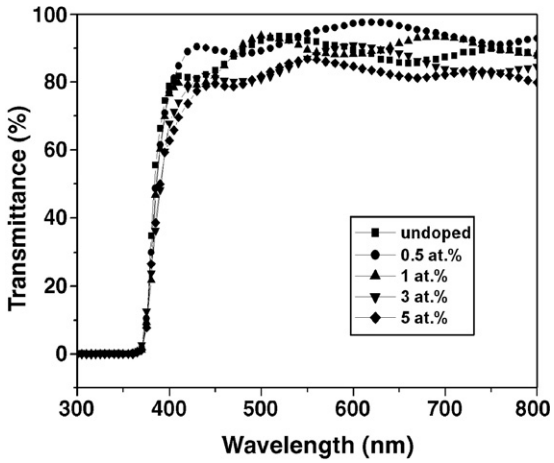

Fig. 4. Optical transmittance spectra of undoped and doped ZnO thin films, the second post-heat treatment with the first post-heat treatment at 550 °C.

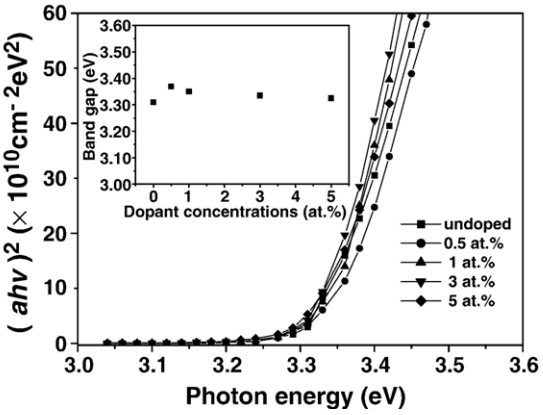

Fig. 5. Plot of $(\alpha h\nu)^2$ versus photon energy for different yttrium-doped ZnO thin films, the second post-heat treatment with the first post-heat treatment at 550 °C.

of oxygen in the grain boundaries which act as traps for the carriers [22].

3.4. Optical properties

Fig. 4 shows the optical transmittance spectra with wavelengths from 300 to 800 nm of the undoped and doped ZnO thin films after the second post-heat treatment with the first post-heat treatment at 550 °C. The fluctuation in the transmission spectrum is due to the interferences in the thin film owing to the reflection at the air–ZnO and ZnO–silica glass interfaces [23]. The films were found to be transparent in the visible range with a sharp absorption edge at wavelengths of about 375 nm, which is very close to the intrinsic band gap of ZnO (3.30 eV). The average optical transmittance values of these annealed films were more than 80% in the visible range. In particular, the transmittance of the 0.5 at.% yttrium-doped film was higher than 90% in the visible range.

The absorption coefficient α was calculated by

$$T = (1-R)^2\exp(-\alpha d), \quad (1)$$

where T is the transmittance of the thin film, R is its reflectivity, and d is the film thickness. The optical band gaps of the films were determined by applying the Tauc model [24] and David and Mott [25] in the high absorbance region:

$$\alpha h\nu = D(h\nu - E_g)^n, \quad (2)$$

where $h\nu$ is the photon energy, E_g is the optical band gap and D is constant. For a direct transition, $n=1/2$ or 2/3 and the former value was found to be most suitable for ZnO thin films, since it gives the best linear graph in the band edge region [26]. The variations of $(\alpha h\nu)^2$ versus the photon energy $h\nu$ in the fundamental absorption region are plotted in Fig. 5. Extrapolation of linear portion to the energy axis at $(\alpha h\nu)^2=0$ gives the E_g value. The band gap of ZnO thin films was increased from 3.30 eV for the undoped films to 3.37 eV for yttrium doping. The band gap of yttrium-doped ZnO thin films is larger than the undoped thin films, which may be explained by the Burstein-Moss shift [27]. That is, the Fermi level was lifted into the conduction band of the degenerated semiconductor when ZnO thin films were doped with yttrium, which leads to the energy band broadening (blue shift) effect.

4. Conclusions

Yttrium-doped ZnO thin films were prepared by sol–gel method. The films deposited at the first post-heat treatment temperature showed preferred ZnO (0 0 2) orientation, while the intensity of a (0 0 2) peak increased with an increase in the annealing temperature. Surface morphologies of the 0.5 at.% yttrium-doped ZnO thin films showed a particulate and porous structure. Also, the cross-section image of a film showed a columnar structure and a thickness of about 300 nm. After the second post-heat treatment with the first post-heat treatment at 550 °C, the 0.5 at.% yttrium-doped film reached the lowest electrical resistivity of 6.75×10^{-3} Ω cm, while a transmittance of over 90% in the visible range was achieved. The energy band gap of ZnO thin films calculated from the transmittance spectra is about 3.30–3.37 eV.

References

[1] H. Sato, T. Minami, Y. Tamura, S. Sakata, T. Mori, N. Ogawa, Thin Solid Films 246 (1994) 86.
[2] M. Chen, Z.L. Pei, C. Sun, J. Gong, R.F. Huang, L.S. Wen, Mater. Sci. Eng., B, Solid-State Mater. Adv. Technol. 85 (2001) 212.
[3] T. Pauporté, D. Lincot, Electrochim. Acta 45 (2000) 3345.
[4] R. Banerjee, S. Ray, N. Basu, A.K. Batabyal, A.K. Barua, J. Appl. Phys. 62 (1987) 912.
[5] H. Ko, W.-P. Tai, K.-C. Kim, S.-H. Kim, S.-J. Suh, Y.-S. Kim, J. Cryst. Growth 277 (2005) 352.
[6] J.B. Lee, S.H. Kwak, H.J. Kim, Thin Solid Films 423 (2003) 262.
[7] J.-L. Zhao, X.-M. Li, J.-M. Bian, W.-D. Yu, X.-D. Gao, J. Cryst. Growth 276 (2005) 507.
[8] J. Hu, R.G. Gordon, J. Appl. Phys. 71 (1992) 880.
[9] S.T. Tan, B.J. Chen, X.W. Sun, X. Hu, X.H. Zhang, S.J. Chua, J. Cryst. Growth 281 (2005) 571.
[10] R. Al Asmar, J.P. Atanas, M. Ajaka, Y. Zaatar, G. Ferblantier, J.L. Sauvajol, J. Jabbour, S. Juillaget, A. Foucaran, J. Cryst. Growth 279 (2005) 394.
[11] P. Nunes, E. Fortunato, R. Martins, Thin Solid Films 383 (2001) 277.
[12] R. Ayouchi, F. Martin, D. Leinen, J.R. Ramos-Barrado, J. Cryst. Growth 247 (2003) 497.
[13] Y.S. Kim, W.P. Tai, S.J. Shu, Thin Solid Films 491 (2005) 153.
[14] M. Ohyama, H. Kozuka, T. Yoko, J. Am. Ceram. Soc. 81 (1998) 1622.
[15] K.Y. Cheong, N. Muti, S.R. Ramanan, Thin Solid Films 410 (2002) 142.
[16] E.J. Luna-Arredondo, A. Maldonado, R. Asomoza, D.R. Acosta, M.A. Meléndez-Lira, M. de la L. Olvera, Thin Solid Films 490 (2005) 132.
[17] M. Ohyama, H. Kozuka, T. Yoko, Thin Solid Films 306 (1997) 78.
[18] J.-H. Lee, B.-O. Park, Thin Solid Films 426 (2003) 94.
[19] V. Fathollahi, M. Mohammadpour Amini, Mater. Lett. 50 (2001) 235.
[20] M. Berber, V. Bulto, R. Kliβ, H. Hahn, Scripta Mater. 53 (2005) 547.
[21] J.-H. Lee, K.-H. Ko, B.-O. Park, J. Cryst. Growth 247 (2003) 119.
[22] S. Major, A. Banerjee, K.L. Chopra, Thin Solid Films 122 (1984) 31.
[23] H. Li, J. Wang, H. Liu, H. Zhang, X. Li, J. Cryst. Growth 275 (2005) e943.
[24] J. Tauc, Amorphous and Liquid Semiconductors, Plenum, London, 1974.
[25] E.A. David, N.F. Mott, Phila. Mag. 22 (1970) 903.
[26] S.T. Tan, B.J. Chen, X.W. Sun, W.J. Fan, J. Appl. Phys. 98 (2005) 013505.
[27] E. Burstein, Phys. Rev. 93 (1954) 632.